

PAPER • OPEN ACCESS

Effect of crystallization time on the structure of the Aluminosilicate glass-ceramic

To cite this article: R Souag *et al* 2018 *J. Phys.: Conf. Ser.* **1081** 012003

View the [article online](#) for updates and enhancements.



The Electrochemical Society
Advancing solid state & electrochemical science & technology

240th ECS Meeting ORLANDO, FL

Orange County Convention Center Oct 10-14, 2021



Abstract submission due: April 9

SUBMIT NOW

Effect of crystallization time on the structure of the Aluminosilicate glass-ceramic

R Souag¹, N Kamel², D Moudir², Y Mouheb² and S Kamariz²

¹URMPE, Research Unit for Materials, Processes and Environment, Faculty of Engineering Sciences, University M'hamed Bougara Boumerdes, 35000, Boumerdes, Algeria

²Nuclear Research Center of Algiers, Nuclear Technology Division, 2. Bd Frantz Fanon, BP 399, RP-Algiers.

E-mail: souagrafika@yahoo.fr

Abstract. All This study deals with the influence of the time of crystallization on the structure of an aluminosilicate glass-ceramic ceramized by a nucleation –crystallization treatment at 790°C for 2 h, and 900°C, for different periods of time ranging from 2 to 12 h. For the whole of the materials, Archimedes density is between 2441-2578 kg/m³. Both X-ray diffraction and scanning electron microscopy analyses reveal two main crystalline phases for the whole of the heating treatments, namely spodumene and leucite. These phases grow regularly with the crystallization time. In addition, aqueous stability testing was carried out using the standard MCC-2 static leach test method at 90 °C and V(ml) = 30 S(cm²) for a series of five test durations - 7, 14, 28, 35 and 42 days. The X-ray fluorescence analytical technique was used to determine the concentration of lanthanum (La) and molybdenum (Mo) leached in our material. The dissolution parameters, in this case the normalized elemental mass loss (NL) and the leaching rate (τ) of each element, were determined from these concentrations. The results demonstrate that The leaching tests showed that the material is stable and it stabilizes at low values ($2.5 \cdot 10^{-9}$ Kg/m²) for La when the ceramization time does not exceed 4h beyond this, Leaching equilibrium and the passivation phase is broken. For Mo and for all glass ceramics at different times of crystallization, the equilibrium reaches ($3.15 \cdot 10^{-8}$ Kg/m²j) and the passivation layer is formed. The glass ceramics at different time of cristallization presently studied appears to have a good chemical durability.

1. Introduction

Glass-ceramics (GC) containing highly durable crystalline particles homogeneously dispersed in the bulk of a glass matrix have been proposed as important candidates for the immobilization of high level radioactive wastes (HLW). They show potential interest to the confinement of radioactive waste by presenting a double shell protection, the first envelope is the crystalline phase, which traps radionuclides, and the second one is the glass as a second barrier surrounding the crystal [1]. In this context, glass-ceramics matrices constituted by crystals distributed homogeneously within a glass matrix and exhibiting increased performances (chemical durability and capacity of reception) compared with the aluminoborosilicate glasses currently used to confine all the waste are particularly interesting [2-5]. This study deals with the influence of the time of crystallization on the structure of an aluminosilicate glass-ceramic ceramized by a nucleation –crystallization treatment at 790°C for 2 h, and 900°C, for different



periods of time ranging from 2 to 12 h. The influence of the time of crystallization (t_c) on the nature of the crystalline phases formed in the bulk of the material is studied. In addition, aqueous stability testing was carried out using the standard MCC-2 static leach test method at 90 °C.

2. Experimental

The GC chemical composition is given in table 1. The following commercial reagents are used for the synthesis: Al₂O₃ (FLUKA), Fe₂O₃ (MERCK, Purity ≥99%), Na₂O (Merck, purity≥99.5%), K₂O (MERCK, Purity≥99%), Li₂O (MERCK, Purity ≥ 99%), MgO (FLUKA, Purity ≥ 97%), MoO₃ (MERCK, Purity≥99.5%), SiO₂ (Prolabo), ZrO₂ (Aldrich, Purity≥ 99%) and Y₂O₃ (MERCK, Purity≥99%). The rare earth oxides are dried at 1000 °C, and the other oxides at 400 °C overnight. This step is important to ensure homogeneity of synthetic products, and obtain materials with isotropic properties.

La₂O₃ is prepared by calcination at 450 °C from La (NO₃)₃ 6 H₂O (Fluka, purity≥99.99%). All reagents are finely ground in a manual agate mortar to obtain a particle size of about 20 μm before the preparation of the mixtures.

Table 1. Chemical composition (in molar %.) of the based glass per 100 g of mixture.

Oxides	ZrO ₂	Al ₂ O ₃	MgO	Na ₂ O	Fe ₂ O ₃	K ₂ O	Li ₂ O	La ₂ O ₃	Y ₂ O ₃	MoO ₃	SiO ₂	Total
Molar %	4.5	15.0	5.0	6.0	2.0	2.9	12.0	0.5	0.5	0.5	48.6	100.0

The powder mixtures are homogenized in an Automatic Sieve Shaker D403 shaker for 6 h, to ensure good dispersion of the mixture. Both nucleation and crystallization temperatures are deducted from trace DTA (differential thermal analysis) analysis of the parent glass. Nucleation is carried out in the same furnace as that used for the glass melting of the oxide mixture at a nucleation temperature (T_n) such as: $T_n = T_g + 20$, thus 790 °C, for 2 h. Grain growth can be performed at a temperature close to the crystallization temperature of the base glass, T_c , which is 900 °C. The crystallization time (t_c) is optimized as following: 6, 9 and 12 h. The GCs are cooled in open air to room temperature. The powders densities (ρ_A) are measured by the Archimedes method. XRD analysis of the materials is performed by a Philips X'Pert Pro diffractometer, with Cu K α 1 ray ($\lambda = 1.5418$ Å), using Philips X'Pert High Score software for phase identification [6].

A scanning electron microscope (SEM) Philips XL30 allowed micrographic observations. Aqueous stability testing was carried out using the standard MCC-2 static leach test method at 90 °C and $V(\text{ml}) = 30 S(\text{cm}^2)$ for a series of five test durations - 7, 14, 28, 35 and 42 days.

The X-ray fluorescence (XRF) technique is used to measure the Lanthane (La) and Molybdene (Mo) dissolution rate in all the aqueous leachates. The employed XRF spectrometer is a Magix-Pro PAN Analytical equipment.

The normalized elemental mass loss in this solution (NL) is defined by the following relationship:

$$NL = C_i \cdot V_o / S_o \cdot F_i \quad (1)$$

With:

C_i : is the total concentration of La or Mo leached ($\text{kg} \cdot \text{m}^{-3}$),

V_o : the total volume of the leaching mixture (m^3),

S_o : the sample initial surface in actual contact with the leachate (m^2),

F_i : the La or Mo weight fraction in the material,

And the normalized leaching rate is expressed by the relation:

$$\tau i = \left(\frac{1}{Fi} + So \right) * \left(\frac{dmi}{\Delta t} \right) \quad (2)$$

With:

τi : the normalized leaching rate of la or Mo, expressed by $\text{kg.m}^{-2}.\text{j}^{-1}$

m_i : the leached mass of La or Mo during a time interval Δt expressed in kg,

Δt : is the interval time leach (j),

3. Results and Discussions

The density of the obtained GCs with different crystallization times (t_c) is measured by the Archimedes method. The results are given in Table 2.

Table 2. Variation of the GC densities (kg/m^3) according to crystallization time (h).

Cristallisation time t_c (h)	2	4	6	9	12
Density ρ_A (kg/m^3)	2441	2492	2509	2532	2573

The GC density increases with the crystallization time. It is between 2441 and 2573 kg/m^3 for all the materials. This density rise can be attributed to the gradual germination and continuous heavy crystalline phases as a function of crystallization time. However, this hypothesis must be confirmed by further investigations of the GCs. Seokju J. and al. [7] report densities values close to our results ($\approx 2.8 \text{ g/cm}^3$) for cordierite glass-ceramics synthesized by a melting at 1450°C and a crystallization and crystal growth treatments, at 750 and 1020°C, respectively.

The GC XRD analysis gave the diffractograms depicted in Figure 1. The results of the phases identification are shown in Table 3.

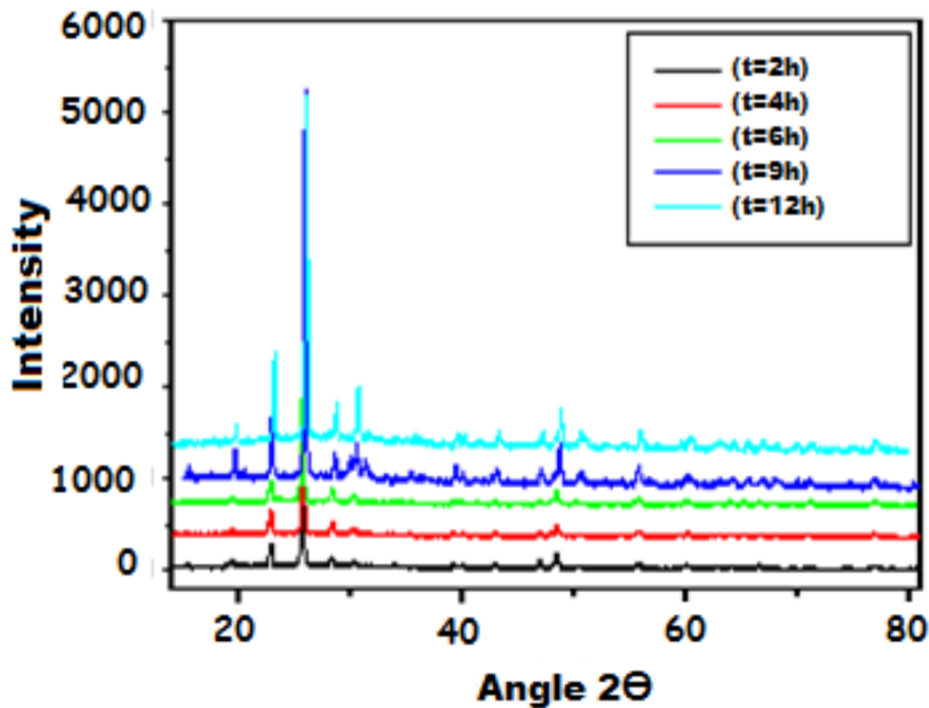


Figure 1. Diffractograms of the GCs for different crystallization times.

We find that for all GCs and at different crystallization times, a major phase of the aluminosilicate type of the pyroxene (Si_2O_6) family, with chemical formula MAlSi_2O_6 ($\text{M} = \text{Li, K, Na or Mg}$) has been identified. This phase is known as a containment barrier against the dissipation of radionuclides, the rate of the formation of this phase increases as with crystallization time increases. At $t_c = 2$ h, this aluminosilicate phase of spodumene nature has already formed at 39%. Two major phases were observed and distributed equally at $t_c = 4$ h, these two phases being a spodumene aluminosilicate with 48% and a molybdate phase with a germination rate of 49% ($15\% \text{Sm}_2(\text{MoO}_4)_3 + 34\% \text{Fe}_2(\text{MoO}_4)_3$). At $t_c = 9$ h, a main aluminosilicate phase of leucite (KAlSi_2O_6) is assigned to the crystallized GC.

This aluminosilicate phase of the pyroxene family crystallizes progressively with the crystallization time to the detriment of the molybdate phase ($\text{NaLa}(\text{MoO}_4)_2$), which reaches 5% at $t_c = 12$ h. The highest aluminosilicate content, but doped in two different ways, is obtained for the maximum crystallization temperature ($t_c = 12$ h). It exceeds 92% ($60\% \text{Mg}_{0.6}\text{Al}_{1.2}\text{Si}_{1.8}\text{O}_6$ and $32\% \text{NaAlSi}_2\text{O}_6$).

Therefore, one can infer that the rise of crystallization time leads to the preferential germination of aluminosilicate phases.

Table 3. The GCs crystalline phases identification for different crystallization times.

Crystallization time (t_c) (h)	Chemical composition	JCPDS data [2]
2	39 % $\text{LiAlSi}_2\text{O}_6$	(01-074-1106)
	48% CaAl_4O_7	(01-076-0706)
	1 % ZrO_2	(01-079-1770)
	12% $\text{Na}_{0.048}(\text{Ca}_{1.53}\text{Y}_{0.47})(\text{Al}_{0.48}\text{Be}_{2.52}\text{Si}_{12}\text{O}_{30})$	(01-080-2240)
4	48% $\text{LiAlSi}_2\text{O}_6$	(01-074-1106)
	3% LiFeO_2	(01-089-2783)
	15% $\text{Sm}_2(\text{MoO}_4)_3$	(00-024-1000)
	34% $\text{Fe}_2(\text{MoO}_4)_3$	(01-072-0935)
6	79 % $\text{LiAlSi}_2\text{O}_6$	(01-074-1106)
	19% $\text{Pr}_2\text{Zr}_3(\text{MoO}_4)_9$	(00-051-1851)
	2% $\text{Zr}_{0.935}\text{Y}_{0.065}\text{O}_{1.968}$	(01-080-2187)
9	82 % KAlSi_2O_6	(01-081-2221)
	11 % $(\text{K}_{2.5}\text{Na}_{0.5})\text{Na}(\text{MoO}_4)_2$	(01-088-0302)
	7 % $\text{Mg}_{1.55}\text{Fe}_{1.6}\text{O}_4$	01-080-0073)
12	60 % $\text{Mg}_{0.6}\text{Al}_{1.2}\text{Si}_{1.8}\text{O}_6$	(01-075-1568)
	32 % $\text{NaAlSi}_2\text{O}_6$	(01-071-1504)
	5 % $\text{NaLa}(\text{MoO}_4)_2$	(00-024-1103)
	3 % $\text{Gd}_3\text{Fe}_2\text{Fe}_3\text{O}_{12}$	(01-072-0141)

The Observation of the microstructure of the studied GCs is carried out by scanning electron microscopy (SEM). The microscope used in this study is Philips ESEM XL 30 equipment. The micrographs are shown in Figures 2.a, 2.b, and 2.c. These micrographs allowed us observing both types of phases: the crystalline and glassy ones, and thus confirm the presence of the main crystalline phases, identified by XRD analysis in the ceramic.

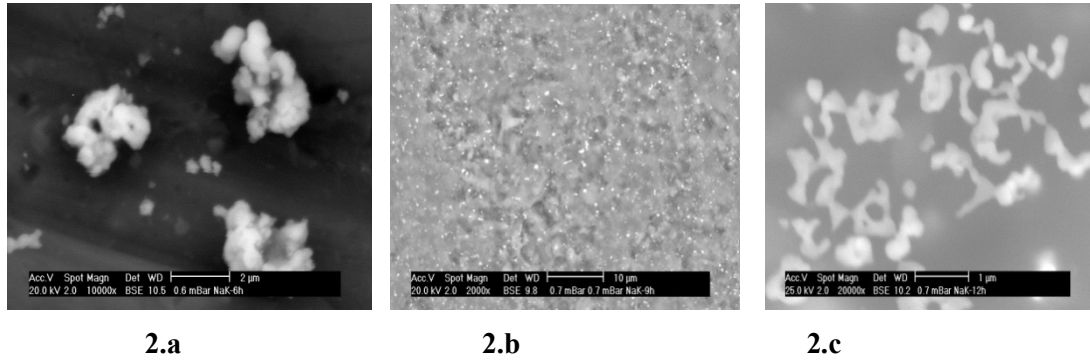


Figure 2. SEM micrographs of the GCs for different T_c values.

The variation of the normalized elemental mass loss (N_L) and the leaching rate of La and Mo (τ_i) are calculated using the formulas (1) and (2) of section 2, respectively.

The results of the evolution of N_L versus time are shown in figure 3, for all the tests.

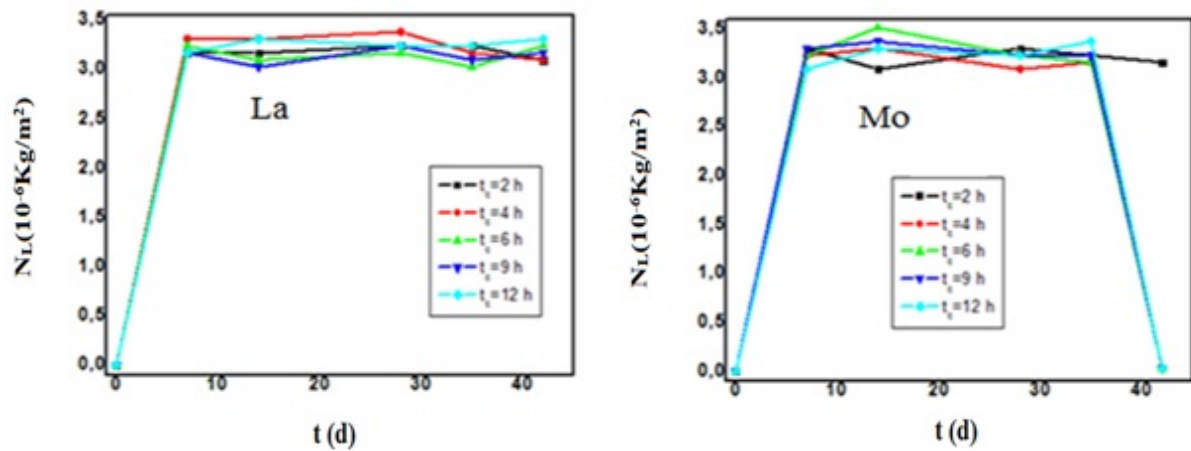


Figure 3. Evolution of the normalized mass loss (10^{-6}Kg/m^2) of La and Mo in leachates, function of time and crystallization time of the GCs.

For all GCs, the normalized mass loss stabilized around $3.10 \cdot 10^{-6}\text{Kg/m}^2$ and 0.410^{-6}Kg/m^2 for La and Mo, respectively; whereas the Mo content is greater than that of La in the base glass, the latter is more releasable than Mo. This proves that lanthanum is probably bound to the glass by weak bonds. It is this fraction which is leached, compared to the small amount of La which is found in the crystalline phases. Especially since the quantities released are larger with the crystallization time (period when a molybdate phase doped with lanthanum appears). The Mo is released with a low content because it is confined in the molybdate phase which appears for all the crystallization times and confirms our results of DRX.

Yong He et al. [8] studied the leaching (MCC1) of an apatite-rich glass-ceramic with a crystallization temperature of 825 and 875 ° C for 2 h. They report $N_L (2.7 \cdot 10^{-6} \text{ Kg/m}^2)$ values for Mo greater than our results obtained for the MCC2 test ($0.41 \cdot 10^{-6} \text{ Kg/m}^2$). This shows that we have a better result despite the aggressive environment we used (90 ° C). For the lanthanum actinide simulator, the value of the

normalized mass loss is $3.10 \cdot 10^{-6} \text{ Kg/m}^2$, which is significantly higher than that found by our previous results ($0.4 \cdot 10^{-6} \text{ Kg/m}^2$) for the leaching of Ce determined from Zr-glass-ceramic ($T_c = 1010^\circ \text{C}$ and $t_c = 2\text{h}$) [9].

The results of the evolution of the La and Mo leaching rate (τ) as a function of time and cristallization time of GCs are gathered in figure 4.

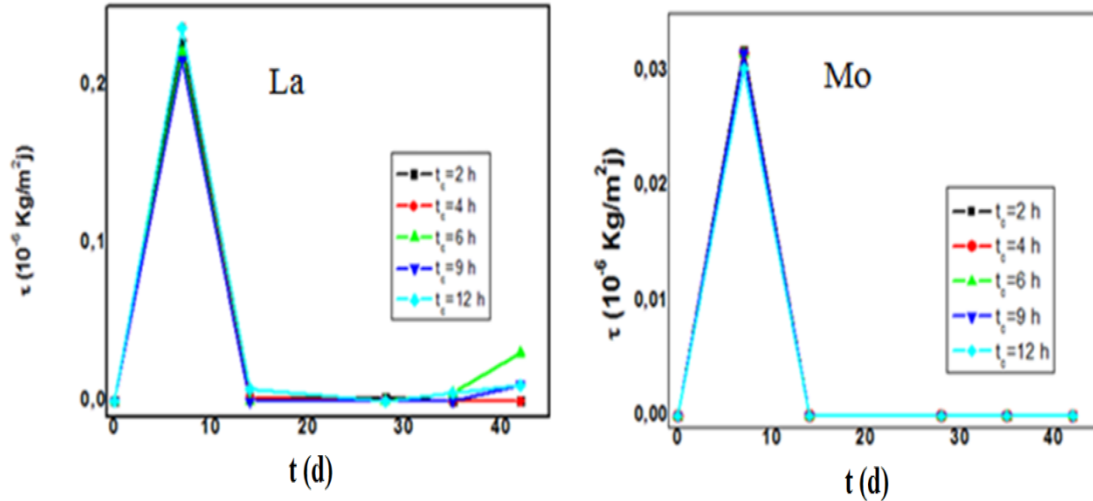


Figure 4. Evolution of the leaching rate ($(10^{-6} \text{ Kg/m}^2\text{j})$) of La and Mo in leachates, function of time and cristallization time of the GCs

The leaching rate in La and Mo increases rapidly to reach a maximum on seventh day and then decreases and stabilizes at low values ($25 \cdot 10^{-10} \text{ Kg / m}^2\text{d}$) for La when the ceramization time does not exceed 4 h. Beyond this, the matrix continues to dissolve for times greater than 35 days, showing that the La is leachable, and therefore is not protected by the spodumene and molybdate ceramics formed and as a result it is dissolved in the glass-ceramics and is weakly Bound to the glass and probably close to the surface thereof. Thus, for a time of ceramization greater than 4 h, there is no leaching equilibrium and the passivation phase is broken beyond 35 days of leaching for La. For Molybdenum and for all Glass-ceramics with different cristallization times, the equilibrium is reached and the passivation layer is formed.

Stéphane Gavarini et al. [10] also carried out a soxhlet dissolution test at $\text{pH} = 5$ of a La and Ce-rich aluminosilicate glass. They report dissolution rates of $(3.5\text{-}6.9) \cdot 10^{-10} \text{ Kg / m}^2$ of La and Ce respectively, after one month (30 days) of testing. These values are very small compared to our values ($25 \cdot 10^{-10} \text{ Kg / m}^2\text{d}$) due may be to the acid medium used by the authors.

As a conclusion, the leaching equilibrium is reached for all the glass-ceramics with a cristallization time greater than 4 h except for the Lanthanum or the passivation phase is broken beyond 35 days of leaching. This shows that our glass-ceramics are durable, and can be recommended as actinide confinement materials.

4. Conclusion

In this study, we performed the synthesis and characterization of glass-ceramic matrices based on an aluminosilicate glass, able to incorporate elements of radioactive waste (fission products and lanthanides) in their structure. The employed synthesis method is the devitrification of a parent glass. It is carried out in several stages: a double fusion of the oxides mixture at 1350°C , a nucleation at 790°C , and a crystal growth at 900°C , for different periods of time ranging from 2 to 12 h. Both X-ray diffraction and scanning electron microscopy analyses reveal two main crystalline phases for the whole of heating treatments, namely spodumene and leucite. These phases grow regularly with the cristallization time. In addition, aqueous stability testing was carried out using the standard MCC-2

static leach test method at 90 °C. The results demonstrate that The leaching tests showed that the material is stable and it stabilizes at low values ($2.5 \cdot 10^{-9} \text{ Kg/m}^2$) for La when the ceramization time does not exceed 4h beyond this, Leaching equilibrium and the passivation phase is broken. For Mo and for all glass ceramics at different times of crystallization, the equilibrium is reached ($3.15 \cdot 10^{-8} \text{ Kg/m}^2$) and the passivation layer is formed. The glass ceramics at different time of cristallization presently studied appears to have a good chemical durability. The studied glass-ceramics have satisfactory mineralogical compositions, because they contain suitable crystalline phases for the double confinement of actinides, such as aluminosilicates (spodumene) and molybdate.

5. References

- [1] Caurant D, 2009 *Nova Science Publishers*, ISBN 978-1-60456-174-6.
- [2] Maddrell E, Thornber S, Hyatt N C 2015 *J. Nucl. Mater.* **456** 461
- [3] Palanivel R and Velraj G 2007 *INDIAN J. PURE & APPL PHYS.* June **45**, 501
- [4] Kaur R, Singh S and Prakash P O, *Physica* 2012 *Physica B* **407** 4765
- [5] Petrovic R, Janackovic D, Zec S, Drmanic S and Kostic-Gvozdenovic L J 2003 *J. Sol-Gel Sci. Technol* **28** 111
- [6] JCPDS data Philips X'Pert High Score Package, 2004, *International Center for Diffraction Data*, Newtown Square PA.
- [7] Seokju J and Seunggu K 2012 *Ceram. Int.* **38S** S543
- [8] Yong H, Weimin B, Chongli S 2002 *J. Nucl. Mater.* **305** 202.
- [9] Souag R 2015 Thèse de doctorat, Université M'Hamed Bougara, Boumerdès, Algeria
- [10] Gavarini S 2003 Thèse de doctorat. Orléans. France